



Mathematical analysis for a new nonlinear measles epidemiological system using real incidence data from Pakistan

Zaibunnisa Memon^{1,a}, Sania Qureshi¹, Bisharat Rasool Memon²

¹ Department of Basic Sciences and Related Studies, Mehran University of Engineering and Technology, Jamshoro, Sindh 76062, Pakistan

² Institute of Information and Communication Technology, University of Sindh, Jamshoro, Pakistan

Received: 17 February 2020 / Accepted: 7 April 2020 / Published online: 28 April 2020

© Società Italiana di Fisica and Springer-Verlag GmbH Germany, part of Springer Nature 2020

Abstract Modeling of infectious diseases is essential to comprehend dynamic behavior for the transmission of an epidemic. This research study consists of a newly proposed mathematical system for transmission dynamics of the measles epidemic. The measles system is based upon mass action principle wherein human population is divided into five mutually disjoint compartments: susceptible $S(t)$ —vaccinated $V(t)$ —exposed $E(t)$ —infectious $I(t)$ —recovered $R(t)$. Using real measles cases reported from January 2019 to October 2019 in Pakistan, the system has been validated. Two unique equilibria called measles-free and endemic (measles-present) are shown to be locally asymptotically stable for basic reproductive number $\mathcal{R}_0 < 1$ and $\mathcal{R}_0 > 1$, respectively. While using Lyapunov functions, the equilibria are found to be globally asymptotically stable under the former conditions on \mathcal{R}_0 . However, backward bifurcation shows coexistence of stable endemic equilibrium with a stable measles-free equilibrium for $\mathcal{R}_0 < 1$. A strategy for measles control based on herd immunity is presented. The forward sensitivity indices for \mathcal{R}_0 are also computed with respect to the estimated and fitted biological parameters. Finally, numerical simulations exhibit dynamical behavior of the measles system under influence of its parameters which further suggest improvement in both the vaccine efficacy and its coverage rate for substantial reduction in the measles epidemic.

1 Introduction

Measles is a highly contagious respiratory disease caused by a virus in the Paramyxoviridae family [1, 2]. Clinical symptoms include high fever, cough, conjunctivitis, rhinitis, Koplik's spots and maculopapular rash. The incubation period for measles is 10–14 days, and the infected individuals usually recover in three weeks of illness without undergoing any complications. However, people suffering from malnutrition or vitamin A deficiency are prone to diarrhea, pneumonia, ear infection, blindness and inflammation of brain [3].

Despite being vaccine preventable, measles continues to pose a serious concern for global health management. The disease has been a primary cause of morbidity and mortality among young children under five years of age. The world has faced measles epidemic several times.

^a e-mail: zaib.memon@faculty.muet.edu.pk (corresponding author)

California faced measles epidemic between 1988 and 1990 with over 16,000 cases and more than 70 deaths reported [4]. In 2018, Madagascar was affected by measles outbreak which infected 50,000 people and resulted in about 300 deaths, majority of them being children [5]. According to World Health Organization (WHO), measles caused more than 140,000 deaths in 2018. Although vaccination has resulted in a 73% drop in measles deaths worldwide between 2000 and 2018, measles is still prevalent in the developing countries in Asia and Africa [6]. The majority of measles-related deaths occur in countries with poor health infrastructures and low per capita incomes.

Pakistan is among the highly measles burdened countries in WHO's Eastern Mediterranean Region [7]. There are recurrent measles outbreaks in the country every 8–10 years. In 2016, there were 2845 confirmed measles cases in Pakistan. This number surged to 6791 in 2017 and 33,007 in 2018. These figures account for about 44%, 20% and 51% of the total number of cases reported in the respective years in the Eastern Mediterranean Region comprising 22 countries. Around 130 children died from the disease in 2017, while the number rose to over 300 in 2018 [8].

Immunization is regarded as one of the most cost-effective and successful public health interventions. The WHO recommends two doses of measles vaccine for all children. The first dose given to infants at nine months provides 85% immunity, while a second dose at the age of twelve months imparts 95% immunity to the disease. A Demographic and Health Survey conducted in Pakistan during 2017–2018 indicated the nationwide coverage of the first and second dose of measles vaccine at 73% and 67%, respectively. The survey illustrated the significant variation in the estimates of vaccine coverage among different provinces and federal areas in the country with Sindh (61%, 60%), Punjab (85%, 82%), Khyber Pakhtunkhwa (63%, 50%), Baluchistan (33%, 34%), Azad Kashmir (83%, 75%), Gilgit Baltistan (66%, 62%) and Federally Administered Tribal Areas (35%, 21%). These figures are well below the WHO recommended coverage of $\geq 95\%$ for both doses of the vaccine [9].

The epidemic models help to describe the mechanism of disease spread and evaluate strategies for the disease control. In recent decades, there has been a growing interest in the use of deterministic compartmental models to study the dynamics of measles and finding ways for its control and prevention. For example, in [10], the authors have taken into account the impact of asymptomatic individuals on measles dynamics. In [11], the authors have shown that wider distancing between measles-infected and non-infected people proves effective in controlling the disease spread. Smith et al. [12] and Peter et al. [14] examined the role of vaccination on measles dynamics. Garba et al. [13] designed a deterministic model to assess the effect of vaccination and treatment on measles transmission. The effect of quarantine and treatment on measles spread is studied in [15]. Other significant contributions can be found in [16–19]. There are a number of case studies found in the literature related to mathematical study of measles, using deterministic models, focusing different regions of the world, for example, Madagascar [20], London [21], China [22, 23], Kenya [24], Cape Coast [25], Ontario [26], Italy [27], Taiwan [28], Senegal [29] and Afghanistan [30].

The objective of present study is to find, via mathematical modeling, a public health strategy based on using vaccine for efficient control of measles in Pakistan. In particular, we aim to analyze the effect of vaccine efficacy and its coverage in preventing the disease spread in the country. Our motivation derives from a few studies [31–34] in the literature focused on deterministic modeling of measles disease in Pakistan. Each of these studies is based on a four-compartmental SEIR (S-susceptible, E-exposed, I-infectious and R-recovered) model, and none investigates the role of vaccine efficiency and its coverage rate on the disease control. The model in this study is an extension of SEIR model that includes a separate

compartment V for the vaccinated class. The SVEIR model is based on the assumption of continuous vaccination. The findings of present study may assist government and public health authorities in formulating strategic vaccination plans to deal with the immunization gaps and thus prevent measles outbreaks.

This paper is organized as follows. In Sect. 2, model is formulated and estimates are obtained for the model parameters. Model equilibria are obtained in Sect. 3 along with analysis of backward bifurcation, local and global stability. Section 4 discusses herd immunity, while a discussion on sensitivity analysis is carried out in Sect. 5. In Sect. 6, numerical simulations are presented to study the effects of various model parameters on the dynamics of measles infection. Conclusion and future research directions are given in Sects. 7 and 8, respectively.

2 Model description

We formulate a deterministic mathematical model comprising five ordinary differential equations. The total population is divided into five compartments that denote the sub-populations: susceptible (*S*), vaccinated (*V*), asymptomatic or exposed (*E*), symptomatic or infectious (*I*) and recovered (*R*). A flow diagram for the model is given in Fig. 1.

The equations describing the model are:

$$\begin{aligned}
 \frac{dS}{dt} &= \Pi - \beta SI - (\xi + \mu)S, \\
 \frac{dV}{dt} &= \xi S - (1 - \tau)\beta VI - \mu V, \\
 \frac{dE}{dt} &= \beta SI + (1 - \tau)\beta VI - (\alpha + \mu)E, \\
 \frac{dI}{dt} &= \alpha E - (\delta + \mu)I, \\
 \frac{dR}{dt} &= \delta I - \mu R,
 \end{aligned}
 \tag{2.1}$$

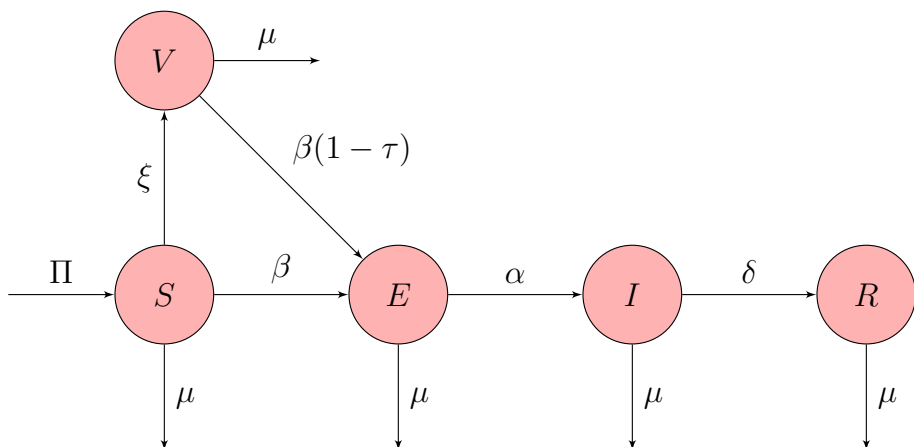


Fig. 1 Flow diagram for measles model specified in (2.1)

with force of infection $\lambda = \beta I$. In (2.1), Π denotes the recruitment rate and keeps the total population N a constant, β the effective contact rate, ξ the vaccination coverage rate, τ the vaccine efficiency, μ the natural mortality rate, α the rate of developing clinical symptoms and δ the recovery rate. In this study, the vaccine is assumed to be imperfect, i.e., it does not provide a 100% prevention of infection. Thus, vaccinated individuals also become infected via contact with symptomatic individuals. Note that, $0 < \tau < 1$ ($\tau = 1$ means perfect vaccine, while $\tau = 0$ represents a vaccine that offers no protection at all). The initial conditions of the model (2.1) are of the form

$$S(0) \geq 0, V(0) \geq 0, E(0) \geq 0, I(0) \geq 0, R(0) \geq 0. \tag{2.2}$$

It can be easily shown that the solution of model (2.1) subject to the initial conditions (2.2) exists and is nonnegative for all $t \geq 0$. Further,

$$\Gamma = \left\{ (S, V, E, I, R) \in \mathbf{R}_+^5 : S(t) + V(t) + E(t) + I(t) + R(t) \leq \frac{\Pi}{\mu} \right\} \tag{2.3}$$

is the positively invariant region for the model (2.1).

2.1 Parameters estimation and curve fitting

One of the most important steps to be taken during model validation is the use of real data (if available) which assists to get values of some unknown biological parameters used in the epidemiological model under study. In this connection, real measles incidence cases as given in Table 1 are used for validation of the proposed measles model and also to obtain best fitted values of some unknown biological parameters that occur in the model. For the model in present research analysis, there are seven parameters among which four are to be fitted, whereas remaining three are estimated such as the natural mortality rate μ of a Pakistani is 66.5 years ($1.253133e-03$ per month) according to WHO data (year-2018) and the population of Pakistan in 2018 is 207862518 and in this way, the recruitment rate is estimated to be $\Pi = 207862518 \times \mu \approx 260479$. Further, it is also known from [35] that the measles vaccine is about 97% effective; therefore, the vaccine efficacy τ is estimated to be 0.97. In addition to these estimated values, values of other parameters are mentioned in Table 2 where the parameters β (contact rate), δ (recovery rate), α (rate of developing clinical symptoms) and ξ (vaccination coverage rate) are obtained through parameter estimation technique under *lsqcurvefit* routine via MATLAB software. The simulation results obtained for the measles incidence cases by fitting the proposed model (2.1) with the real statistics of the first 10 months of 2019 are shown in Fig. 2 along with the respective residuals as depicted in Fig. 3. Figure 2 presents a reasonably good fit thereby including reality to the predictions obtained from the proposed measles model (2.1). The associated average relative error of the fit using the formula $\frac{1}{10} \sum_{k=1}^{10} \left| \frac{x_k^{\text{real}} - x_k^{\text{approximate}}}{x_k^{\text{real}}} \right| \approx 1.4685e - 01$ is used to measure goodness of the fit which is further confirmed by reasonably small relative error's value ($1.4685e-01$).

Table 1 Real statistics of measles infected cases from January to October 2019 in Pakistan [36]

Jan	Feb	Mar	Apr	May	June	July	Aug	Sep	Oct
237	252	397	399	276	168	70	28	23	19

Table 2 Biological parameters used in the proposed epidemic model of measles

Parameter	Description	Value	Source
Π	Recruitment rate of susceptible humans	260,479	Estimated
μ	Natural mortality rate	1.253133e-03	Estimated
τ	Efficacy of vaccine	0.97	Estimated
β	Measles contact rate	1.60056e-07	Fitted
δ	Recovery rate	9.3408	fitted
α	Rate of developing clinical symptoms	9.2373e-01	Fitted
ξ	Vaccination coverage rate	5.8306e-01	Fitted

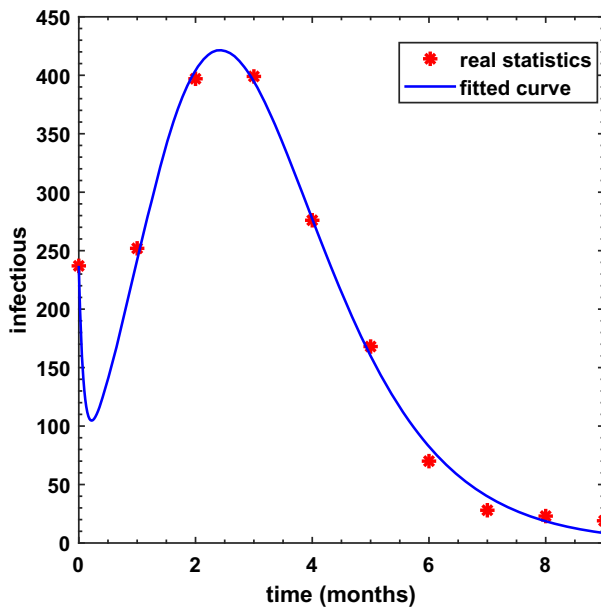


Fig. 2 Fitting the proposed measles model to the real statistical data using parameters from Table 2

3 Equilibria and stability

3.1 Disease-free and endemic equilibrium points

Given that the total population N is a constant, it is possible to obtain disease-free equilibrium X_0 by equating to zero the right side of equations in system (2.1) as

$$X_0 = (S_0, V_0, E_0, I_0, \mathcal{R}_0) = \left(\frac{\Pi}{\xi + \mu}, \frac{\xi \Pi}{\mu(\xi + \mu)}, 0, 0, 0 \right). \tag{3.1}$$

Next, we compute the basic reproductive ratio \mathcal{R}_0 using only the two equations corresponding to compartments E and I from system (2.1) using the next-generation matrix method [37].

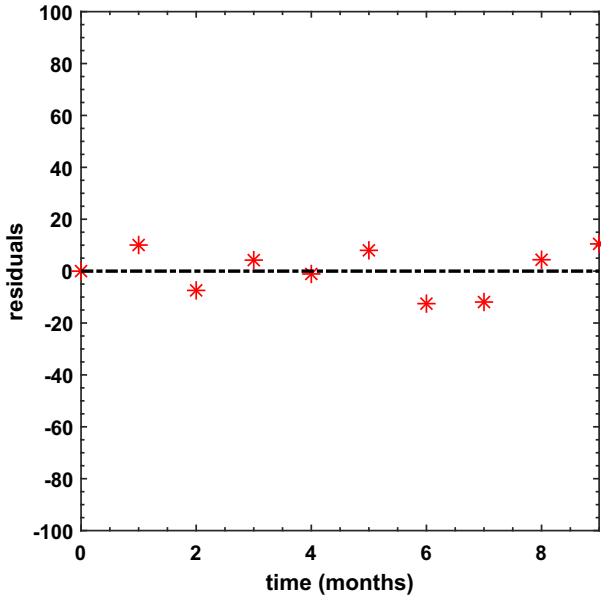


Fig. 3 Residuals for the proposed model using parameters from Table 2

The next-generation matrix is the product of matrices \mathbf{F} and \mathbf{V}^{-1} where the matrix \mathbf{F} represents the rate of infection transmission in these compartments, and the matrix \mathbf{V} describes all other transfers across the compartments. The matrices \mathbf{F} , \mathbf{V} and \mathbf{V}^{-1} are given as

$$\mathbf{F} = \begin{bmatrix} 0 & \frac{\beta\Pi[\mu+(1-\tau)\xi]}{\mu(\xi+\mu)} \\ 0 & 0 \end{bmatrix},$$

$$\mathbf{V} = \begin{bmatrix} \mu + \alpha & 0 \\ -\alpha & \mu + \delta \end{bmatrix},$$

$$\mathbf{V}^{-1} = \begin{bmatrix} \frac{1}{\mu+\alpha} & 0 \\ \frac{\alpha}{(\mu+\alpha)(\mu+\delta)} & \frac{1}{\mu+\delta} \end{bmatrix}.$$

The basic reproductive ratio, defined as the spectral radius of the matrix \mathbf{FV}^{-1} , is obtained as

$$\mathcal{R}_0 = \rho(\mathbf{FV}^{-1}) = \frac{\alpha\beta\Pi[\mu + (1 - \tau)\xi]}{\mu(\xi + \mu)(\mu + \alpha)(\mu + \delta)}. \tag{3.2}$$

It is easy to prove that if $\mathcal{R}_0 > 1$, in addition to the disease-free equilibrium point X_0 , system (2.1) also has an endemic equilibrium point $X_* = (S_*, V_*, E_*, I_*, R_*)$, with

$$\begin{aligned}
 S_* &= \frac{\Pi}{\beta I_* + \xi + \mu}, \\
 V_* &= \frac{\xi \Pi}{(\beta I_* + \xi + \mu)[(1 - \tau)\beta I_* + \mu]}, \\
 E_* &= \frac{\delta + \mu}{\alpha} I_*, \\
 I_* &= \frac{-A_2 + \sqrt{A_2^2 - 4A_1A_3}}{2A_1}, \\
 R_* &= \frac{\delta}{\mu} I_*,
 \end{aligned}
 \tag{3.3}$$

where

$$\begin{aligned}
 A_1 &= \beta^2(1 - \tau), \\
 A_2 &= \beta\mu \left(1 + \frac{(1 - \tau)}{\mu + (1 - \tau)\xi} \left(1 - \mathcal{R}_0 + (1 - \tau)\frac{\xi}{\mu} \right) \right), \\
 A_3 &= \mu(\xi + \mu)(1 - \mathcal{R}_0).
 \end{aligned}
 \tag{3.4}$$

3.2 Backward bifurcation analysis

In this section, we analyze the model (2.1) for backward bifurcation [38, 39]. The phenomenon occurs in models having multiple endemic equilibria for $\mathcal{R}_0 < 1$. Evaluating force of infection λ at the endemic equilibrium yields following quadratic equation:

$$a\lambda^2 + b\lambda + c = 0,
 \tag{3.5}$$

with

$$\begin{aligned}
 a &= 4\beta^2(1 - \tau)^2(\xi + \mu)(\alpha + \mu)(\delta + \mu), \\
 b &= 2\beta^2\mu(1 - \tau)(\xi + \mu)(\alpha + \mu)(\delta + \mu) + 2\beta^2(1 - \tau)^2(\xi + \mu)(\alpha + \mu)(\delta + \mu) - 2\alpha\beta^3\Pi(1 - \tau)^2, \\
 c &= 4\beta^2\mu(1 - \tau)(\xi + \mu)^2(\alpha + \mu)(\delta + \mu)(1 - \mathcal{R}_0).
 \end{aligned}$$

Hence, the following theorem is established:

Theorem 3.1 *The model (2.1) has*

- (i) *a unique endemic equilibrium state if $c < 0$,*
- (ii) *a unique endemic equilibrium if $b < 0$ and $c = 0$ or $b^2 - 4ac = 0$,*
- (iii) *two endemic equilibria if $b < 0, c > 0$ and $b^2 - 4ac > 0$,*
- (iv) *no endemic equilibrium otherwise.*

Clearly, $a > 0$ and $c > 0$ or $c < 0$ according to $\mathcal{R}_0 < 1$ or $\mathcal{R}_0 > 1$, respectively. Note that case (i) of Theorem 3.1 suggests the existence of a unique endemic equilibrium for $\mathcal{R}_0 > 1$. Further, case (iii) of the theorem describes the condition for occurrence of backward bifurcation, i.e., coexistence of a disease-free and an endemic equilibrium point. To determine whether the model (2.1) has this phenomenon, the discriminant of Eq. (3.5) is equated to zero and the resulting equation is solved for critical value of \mathcal{R}_0 , denoted as \mathcal{R}_0^c , given by

$$\mathcal{R}_0^c = 1 - \frac{b^2}{4ak},$$

where $k = \beta^2\mu(1 - \tau)(\xi + \mu)^2(\alpha + \mu)(\delta + \mu)$. Therefore, backward bifurcation occurs for $\mathcal{R}_0^c < \mathcal{R}_0 < 1$.

3.3 Stability of equilibrium points

3.3.1 Local stability

Theorem 3.2 *The disease-free equilibrium X_0 is locally asymptotically stable if $\mathcal{R}_0 < 1$ and unstable if $\mathcal{R}_0 > 1$.*

Proof The Jacobian matrix of the system (2.1) at $X_0 = \left(\frac{\Pi}{\xi + \mu}, \frac{\xi \Pi}{\mu(\xi + \mu)}, 0, 0, 0 \right)$ is

$$J(X_0) = \begin{bmatrix} -(\xi + \mu) & 0 & 0 & \frac{-\beta \Pi}{\xi + \mu} & 0 \\ \xi & -\mu & 0 & \frac{-(1-\tau)\beta \xi \Pi}{\mu(\xi + \mu)} & 0 \\ 0 & 0 & -(\alpha + \mu) & \frac{\beta \Pi(\mu + (1-\tau)\xi)}{\mu(\xi + \mu)} & 0 \\ 0 & 0 & \alpha & -(\mu + \delta) & 0 \\ 0 & 0 & 0 & \delta & -\mu \end{bmatrix}.$$

It is easy to verify that three of the eigenvalues of $J(X_0)$ are $\lambda_1 = -(\xi + \mu) < 0$, $\lambda_2 = \lambda_3 = -\mu < 0$ (recall that $0 \leq \tau \leq 1$ and remaining parameters are nonnegative). The remaining two eigenvalues λ_4 and λ_5 can be obtained from the equation

$$\begin{vmatrix} -(\alpha + \mu) - \lambda & \frac{\beta \Pi(\mu + (1-\tau)\xi)}{\mu(\xi + \mu)} \\ \alpha & -(\mu + \delta) - \lambda \end{vmatrix} = 0,$$

which gives a quadratic equation

$$\lambda^2 + (\alpha + \delta + 2\mu)\lambda + (\alpha + \mu)(\delta + \mu)(1 - \mathcal{R}_0) = 0, \tag{3.6}$$

with λ_4 and λ_5 as its roots satisfying the following:

$$\begin{aligned} \lambda_4 + \lambda_5 &= -(\alpha + \delta + 2\mu) < 0, \\ \lambda_4 \lambda_5 &= (\alpha + \mu)(\delta + \mu)(1 - \mathcal{R}_0). \end{aligned} \tag{3.7}$$

The two conditions stated in (3.7) imply that both λ_4 and λ_5 have negative real parts provided $\mathcal{R}_0 < 1$. This proves stability of X_0 . If $\mathcal{R}_0 > 1$, one of λ_4 and λ_5 has positive real part. In this case, X_0 is unstable. □

Theorem 3.3 *The endemic equilibrium X_* is locally asymptotically stable if $\mathcal{R}_0 > 1$.*

Proof The Jacobian matrix of system (2.1) at $X_* = (S_*, V_*, E_*, I_*, R_*)$ is

$$J(X_*) = \begin{bmatrix} -\beta I_* - (\xi + \mu) & 0 & 0 & -\beta S_* & 0 \\ \xi & -(1-\tau)\beta I_* - \mu & 0 & -(1-\tau)\beta V_* & 0 \\ \beta I_* & (1-\tau)\beta I_* & -(\alpha + \mu) & \beta S_* + (1-\tau)\beta V_* & 0 \\ 0 & 0 & \alpha & -(\mu + \delta) & 0 \\ 0 & 0 & 0 & \delta & -\mu \end{bmatrix}.$$

The characteristic equation for $J(X_*)$ is given by

$$(\lambda + \mu)(\lambda^4 + P_3\lambda^3 + P_2\lambda^2 + P_1\lambda + P_0) = 0, \tag{3.8}$$

where

$$\begin{aligned} P_3 &= \alpha + \delta + \xi + 4\mu + (2 - \tau)\beta I_*, \\ P_2 &= (\alpha + \mu)(\delta + \mu) - \alpha\beta(S_* + (1 - \tau)V_*) + (\xi + (2 - \tau)\beta I_* + 2\mu)(\alpha + \delta + 2\mu) \\ &\quad + (\mu + \xi + \beta I_*)(\mu + (1 - \tau)\beta I_*), \\ P_1 &= (\xi + (2 - \tau)\beta I_* + 2\mu)((\alpha + \mu)(\delta + \mu) - \alpha\beta(S_* + (1 - \tau)V_*)) \\ &\quad + (\mu + \xi + \beta I_*)(\mu + (1 - \tau)\beta I_*)(\alpha + \delta + 2\mu) + \alpha\beta^2(S_* - (1 - \tau)^2V_*)I_*, \\ P_0 &= (\mu + \xi + \beta I_*)(\mu + (1 - \tau)\beta I_*)((\alpha + \mu)(\delta + \mu) - \alpha\beta(S_* + (1 - \tau)V_*)) \\ &\quad + \alpha\beta^2((\xi(1 - \tau) + (1 - \tau)\beta I_* + \mu)S_* - (1 - \tau)^2(\mu + \xi + \beta I_*)V_*). \end{aligned} \tag{3.9}$$

From (3.8), an eigenvalue of $J(X_*)$ is $\lambda = -\mu < 0$. Further, it is easy to verify from the four equations in (3.9) that

$$P_3 > 0, P_0 > 0, (P_3P_2 - P_1)P_1 - P_3^2P_0 > 0.$$

Hence, by Routh–Hurwitz stability criterion, the endemic equilibrium point X_* is locally asymptotically stable for $\mathcal{R}_0 > 1$. □

3.3.2 Global stability

Theorem 3.4 *The disease-free equilibrium X_0 is globally asymptotically stable in Γ if $\mathcal{R}_0 \leq 1$.*

Proof Consider the Lyapunov function

$$L_1 = \alpha E + (\alpha + \mu)I. \tag{3.10}$$

The derivative of this function is

$$\begin{aligned} L'_1 &= (\alpha\beta(S + (1 - \tau)V) - (\alpha + \mu)(\delta + \mu))I, \\ &= (\alpha + \mu)(\delta + \mu)(\mathcal{R}_0 - 1)I. \end{aligned}$$

Clearly, $L'_1 \leq 0$ if $\mathcal{R}_0 \leq 1$ with $L'_1 = 0$ only for $I = 0$. The largest compact invariant set in Γ is the singleton set $\{X_0\}$. Hence, by LaSalle’s invariance principle [40], X_0 is globally asymptotically stable in Γ . □

Theorem 3.5 *The endemic equilibrium X_* is globally asymptotically stable in Γ for $\mathcal{R}_0 > 1$.*

Proof Consider the following function

$$\begin{aligned} L_2 &= S - S_* - S_* \log \frac{S}{S_*} + V - V_* - V_* \log \frac{V}{V_*} + E - E_* - E_* \log \frac{E}{E_*} \\ &\quad + \frac{\alpha + \mu}{\alpha} \left(I - I_* - I_* \log \frac{I}{I_*} \right). \end{aligned} \tag{3.11}$$

Taking derivative of this function, we obtain

$$\begin{aligned}
 L'_2 &= \left(1 - \frac{S_*}{S}\right)S' + \left(1 - \frac{V_*}{V}\right)V' + \left(1 - \frac{E_*}{E}\right)E' + \frac{\alpha + \mu}{\alpha} \left(1 - \frac{I_*}{I}\right)I', \\
 &= \left(1 - \frac{S_*}{S}\right) \left[\Pi - \beta SI - (\xi + \mu)S \right] \\
 &\quad + \left(1 - \frac{V_*}{V}\right) \left[\xi S - (1 - \tau)\beta VI - \mu V \right] \\
 &\quad + \left(1 - \frac{E_*}{E}\right) \left[\beta SI + (1 - \tau)\beta VI - (\alpha + \mu)E \right] \\
 &\quad + \frac{\alpha + \mu}{\alpha} \left(1 - \frac{I_*}{I}\right) \left[\alpha E - (\delta + \mu)I \right].
 \end{aligned}$$

It may be noted that

$$\begin{aligned}
 \Pi &= \beta I_* S_* + \xi S_* + \mu S_*, \quad \xi S_* = (1 - \tau)\beta V_* I_* + \mu V_*, \\
 \alpha E_* &= (\delta + \mu)I_*, \quad (\alpha + \mu)E_* = \beta I_* S_* + (1 - \tau)\beta V_* I_*.
 \end{aligned}
 \tag{3.12}$$

Substituting the equilibrium relations from (3.12) in the above expression for L'_2 , we obtain

$$\begin{aligned}
 L'_2 &= \mu S_* \left[2 - \frac{S_*}{S} - \frac{S}{S_*} \right] + \mu V_* \left[3 - \frac{S_*}{S} - \frac{V}{V_*} - \frac{V_* S}{V S_*} \right] + \beta I_* S_* \left[3 - \frac{S_*}{S} - \frac{I_* E}{I E_*} - \frac{I_* S E_*}{I S_* E} \right] \\
 &\quad + (1 - \tau)\beta V_* I_* \left[4 - \frac{S_*}{S} - \frac{S V_*}{S_* V} - \frac{I_* E}{I E_*} - \frac{I V E_*}{I_* V_* E} \right].
 \end{aligned}
 \tag{3.13}$$

Using the inequality of arithmetic and geometric means, one can show that

$$\begin{aligned}
 2 - \frac{S_*}{S} - \frac{S}{S_*} &\leq 0, \\
 3 - \frac{S_*}{S} - \frac{V}{V_*} - \frac{V_* S}{V S_*} &\leq 0, \\
 3 - \frac{S_*}{S} - \frac{I_* E}{I E_*} - \frac{I_* S E_*}{I S_* E} &\leq 0, \\
 4 - \frac{S_*}{S} - \frac{S V_*}{S_* V} - \frac{I_* E}{I E_*} - \frac{I V E_*}{I_* V_* E} &\leq 0.
 \end{aligned}
 \tag{3.14}$$

From (3.13) and (3.14), it follows that $L'_2 \leq 0$ for $\mathcal{R}_0 > 1$. Furthermore, the equality holds if and only if $S = S_*, V = V_*, \frac{I_*}{I} = \frac{E}{E_*}$. Substituting $S = S_*$ in the first equation of (2.1), we get $V = V_*, I = I_*, E = E_*$ and thus $R = R_*$. Hence, by LaSalle’s invariance principle [40], $(S, V, E, I, R) \rightarrow (S_*, V_*, E_*, I_*, R_*)$ as $t \rightarrow \infty$. Therefore, X_* is globally asymptotically stable in Γ for $\mathcal{R}_0 > 1$. \square

4 Herd immunity

Not everyone in a given population needs to be immunized in order to eliminate the disease. The fraction of individuals with immunity in the population required to prevent an epidemic is called herd immunity. Let ρ denote the fraction of population which is vaccinated at X_0 (the disease-free equilibrium). Then,

$$\rho = \frac{V_0}{N_0} = \frac{\xi}{\xi + \mu}.$$

Table 3 Percent values of ρ_c corresponding to various values of τ and \bar{R}_0

τ	\bar{R}_0						
	12	13	14	15	16	17	18
0.95	96.5	97.2	97.7	98.2	98.7	99.1	99.4
0.97	94.5	95.2	95.7	96.2	96.6	97.0	97.4
0.99	92.6	93.2	93.8	94.3	94.7	95.1	95.4

In the absence of vaccination, i.e., when $\xi = 0$, the basic reproductive number given in (3.2) reduces to

$$\bar{R}_0 = \frac{\alpha\beta\Pi}{\mu(\mu + \alpha)(\mu + \delta)}.$$

Hence, we can write

$$\mathcal{R}_0 = \bar{\mathcal{R}}_0 \left(\frac{\mu + (1 - \tau)\xi}{\xi + \mu} \right) = \bar{\mathcal{R}}_0(1 - \rho\tau). \tag{4.1}$$

It must be noted that $\mathcal{R}_0 \leq \bar{\mathcal{R}}_0$. The equality holds only when $\rho = 0$ (i.e., $\xi = 0$) or $\tau = 0$. This implies that the vaccine, even not 100% efficient, will certainly diminish the basic reproductive number of the disease. As $\mathcal{R}_0 \leq 1$ is a necessary and sufficient condition for the elimination of measles (Theorems 3.2 and 3.4), it follows from Eq. (4.1) that

$$\rho \geq \frac{1}{\tau} \left(1 - \frac{1}{\bar{\mathcal{R}}_0} \right) = \rho_c \tag{4.2}$$

is also a necessary and sufficient condition for measles control. Here, ρ_c denotes herd immunity. Combining Theorems 3.2 and 3.4, we get the following result:

Corollary 4.1 *Measles can be eliminated from the population if $\rho \geq \rho_c$.*

Table 3 illustrates the threshold values for the herd immunity ρ_c subject to different values for τ and $\bar{\mathcal{R}}_0$. For instance, if $\bar{\mathcal{R}}_0 = 14$ and $\tau = 0.97$, this implies that at least 95.7% of the population must be vaccinated in order to be a measles-free community. This highlights the equally important roles of vaccine efficiency and the vaccinated proportion of population in the disease control. It further suggests that both these parameters must be significantly high for the disease to be eliminated.

5 Sensitivity analysis of \mathcal{R}_0

As the initial transmission and persistence of a disease are both dependent on the basic reproductive number \mathcal{R}_0 , we perform a sensitivity analysis to identify the model parameters that have the greatest and the least impact on \mathcal{R}_0 . There are various techniques available to carry out the required sensitivity analysis including the sensitivity heat map method [41], scatter plots [42], Latin hypercube sampling–partial rank correlation coefficient [43], the Morris [44] and Sobol’ [45] methods and the normalized forward sensitivity index technique [46]. In the present study, this is done by computing sensitivity indices of \mathcal{R}_0 known as normalized forward sensitivity indices using the following formula:

Table 4 Sensitivity indices for \mathcal{R}_0

Parameters	Sensitivity indices
Π	+1
μ	-0.936782
τ	-30.1718
β	+1
δ	-0.999866
α	0.00135476
ξ	-0.0647072

$$\Gamma_{\theta}^{\mathcal{R}_0} = \frac{\partial \mathcal{R}_0}{\partial \theta} \times \frac{\theta}{\mathcal{R}_0}, \tag{5.1}$$

where θ denotes the model parameter. It has been observed that the basic reproduction number is highly sensitive to the efficacy of vaccine that requires the most attention in order to stop the spread of measles epidemic. On the other hand, the parameter α (rate of developing clinical symptoms) is observed to be least effective parameter toward the basic reproduction number during forward sensitivity analysis. The sensitivity index of \mathcal{R}_0 with respect to each parameter in the model (2.1) is given in Table 4.

$$\begin{aligned} \Gamma_{\Pi}^{\mathcal{R}_0} &= +1 > 0, \\ \Gamma_{\mu}^{\mathcal{R}_0} &= \frac{\alpha}{\alpha + \mu} + \frac{\delta}{\delta + \mu} + \frac{\mu \xi \tau}{(\mu + \xi)(\mu - \xi \tau + \xi)} - 3 < 0, \\ \Gamma_{\tau}^{\mathcal{R}_0} &= -\frac{\xi \tau}{\mu + \xi(1 - \tau)} < 0, \\ \Gamma_{\beta}^{\mathcal{R}_0} &= +1 > 0, \\ \Gamma_{\delta}^{\mathcal{R}_0} &= -\frac{\delta}{\delta + \mu} < 0, \\ \Gamma_{\alpha}^{\mathcal{R}_0} &= +\frac{\mu}{\alpha + \mu} > 0, \\ \Gamma_{\xi}^{\mathcal{R}_0} &= -\frac{\mu \xi \tau}{(\mu + \xi)(\mu + \xi(1 - \tau))} < 0. \end{aligned} \tag{5.2}$$

6 Numerical simulations and discussion

Various numerical simulations are carried out in this section to observe impacts of different biological parameters on the proposed measles model (2.1). In Fig. 4, the burden of the measles epidemic is observed to have declining behavior if the vaccination coverage rate (ξ) is improved, whereas this burden is substantially reduced for reasonably small value of the measles contact rate (β) as shown in Fig. 5. However, these measures are not easy to be taken in a developing country like Pakistan. Therefore, an effective step could be the improvement in the efficacy of the vaccine (τ) which reduces the burden of the epidemic as shown in Fig. 6, but the government of Pakistan will have to strive for making the vaccine cost-effective in order to be affordable by people living near the poverty line. On the other hand, improvement

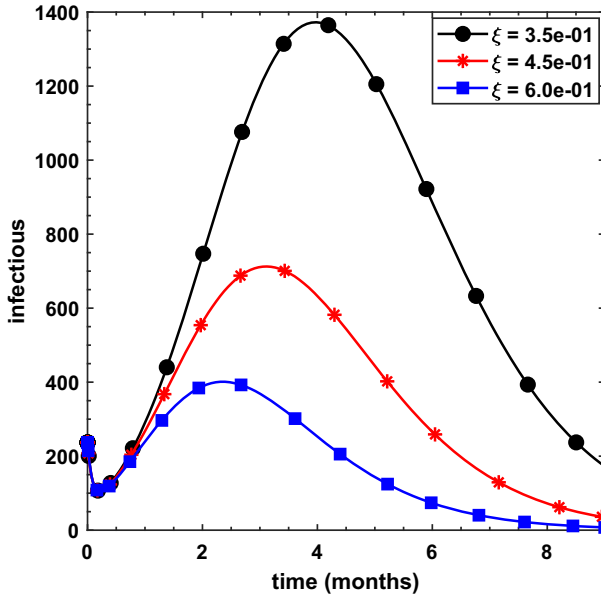


Fig. 4 Dynamical behavior of infectious population for increasing values of vaccination coverage rate (ξ) while using parameters from Table 2

in the recovery rate (δ), as shown in Fig. 7, does reduce the epidemic’s burden, but this measure is not as effective as taking efforts to reduce contacts among infectious and the susceptible ones. Moreover, the higher the rate of developing clinical symptoms (α) more will be the number of infectious individuals as theoretically predicted. This theoretical observation is further confirmed by the infectious population in Fig. 8, but the infection seems to vanish as time goes by.

In order to further support the analysis and observation regarding the proposed measles model (2.1), contour plots (Figs. 9, 10, 11 and 12) for the basic reproductive number are obtained as function of some biological parameters wherein the contact rate (β) is kept on the vertical axis in an increasing fashion and the parameters $\tau, \xi, \delta, \alpha$ are set on the horizontal axis with their increasing values. The most significant observation from these contour plots is that the burden of the measles epidemic can effectively be reduced by reasonably increasing the values of $\tau, \xi, \delta, \alpha$ among which the vaccine’s efficacy (τ) and vaccine’s coverage rate (ξ) play important roles. Finally, the small value for the vaccine’s coverage rate (ξ) is not as bad as the equally small value of the vaccine’s efficacy (τ) as depicted in Fig. 13; however, larger value of (τ) is capable enough to bring \mathcal{R}_0 straight toward 0, whereas \mathcal{R}_0 is not exactly 0 even for the maximum value of (ξ). Thus, the vaccine’s efficacy (τ) plays the most significant role to reduce the burden of the measles epidemic.

7 Conclusion

These research findings are about development of a new continuous time-invariant system for the measles epidemic under vaccination approach. In this regard, we divided the popu-

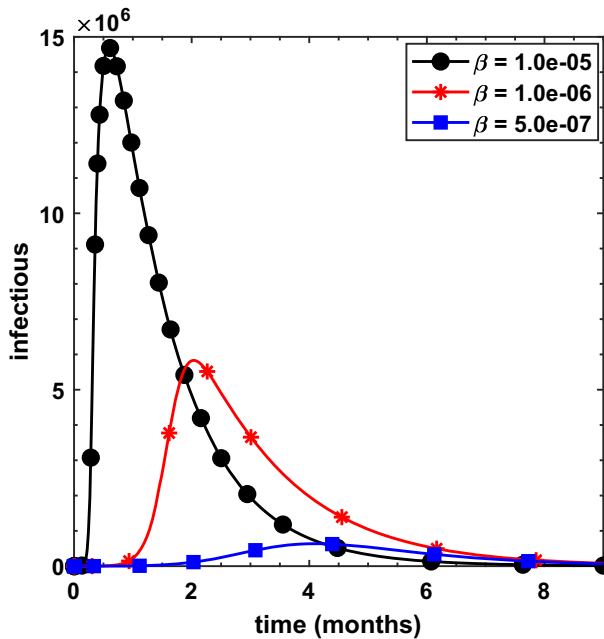


Fig. 5 Dynamical behavior of infectious population for decreasing values of measles contact rate (β) while using parameters from Table 2

lation into five classes of susceptible, vaccinated, exposed, infectious and recovered human population. Parameters involved in the system are obtained with assistance of parameter estimation technique under nonlinear least squares fitting strategy which later produced best fitted curve for the infectious class of the system to the curve of real experimental measles cases obtained from WHO from the month January 2019 to October 2019, in Pakistan. Thus, the proposed measles system is validated having reasonably small relative error value of $1.4685e-01$.

Two unique steady-state solutions are computed for the measles system which are shown to be locally and globally asymptotically stable via Routh–Hurwitz stability theory and Lyapunov functions, respectively, under different constraints imposed upon \mathcal{R}_0 . Thus, the epidemic is said to have died out for $\mathcal{R}_0 < 1$, whereas it persists in the case when $\mathcal{R}_0 > 1$. In addition, the measles system undergoes backward bifurcation wherein a stable endemic equilibrium is found to coexist with a stable measles-free equilibrium for $\mathcal{R}_0 < 1$. The minimum fraction of population that must be vaccinated to achieve herd immunity is determined which shows that both the vaccine efficiency and the vaccinated fraction must be sufficiently high for elimination of measles. The sensitivity analysis shows that the parameter for vaccine efficacy (τ) is the one taken to be care of which is further confirmed in various numerical simulations carried out. In addition, there is need to attain higher vaccine coverage rate which is vital to preventing the disease spread. Hence, vaccine efficacy and its coverage both seem to have substantially positive roles for effective control and elimination of measles burden in the suffering community.

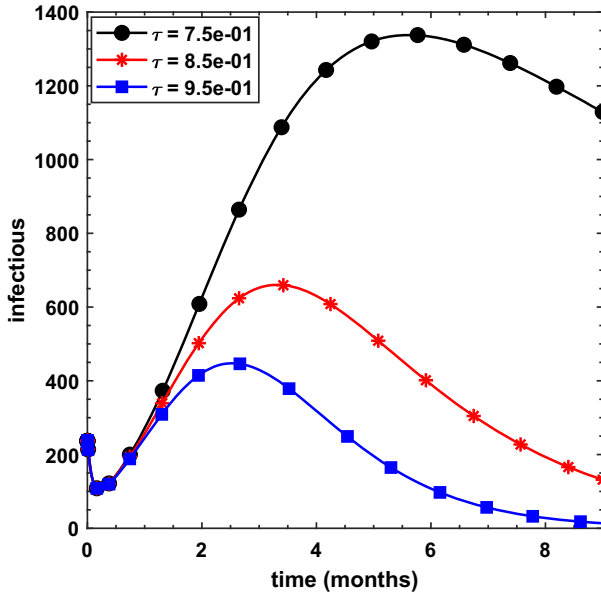


Fig. 6 Dynamical behavior of infectious population for increasing values of vaccine efficacy (τ) while using parameters from Table 2

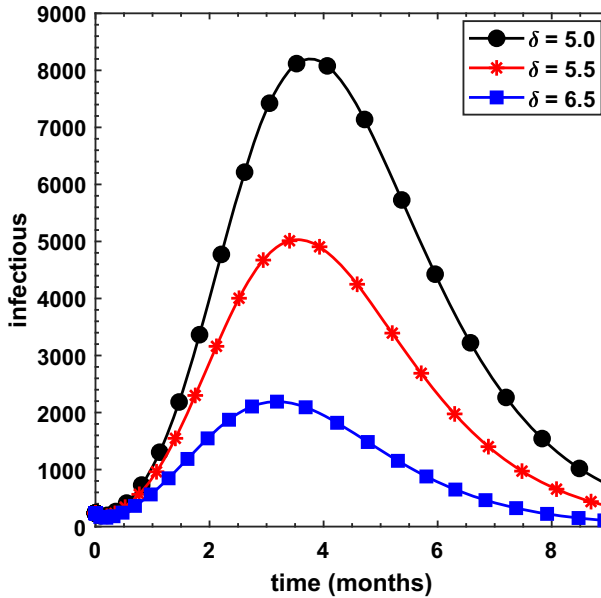


Fig. 7 Dynamical behavior of infectious population for increasing values of recovery rate (δ) while using parameters from Table 2

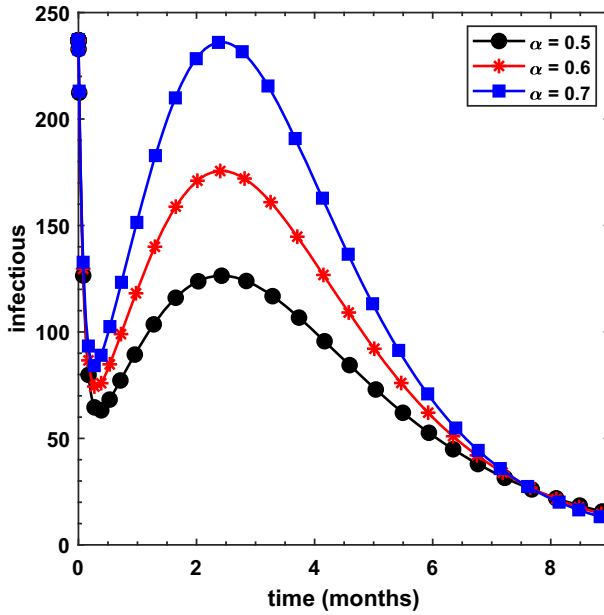


Fig. 8 Dynamical behavior of infectious population for increasing values of rate of developing clinical symptoms (α) while using parameters from Table 2

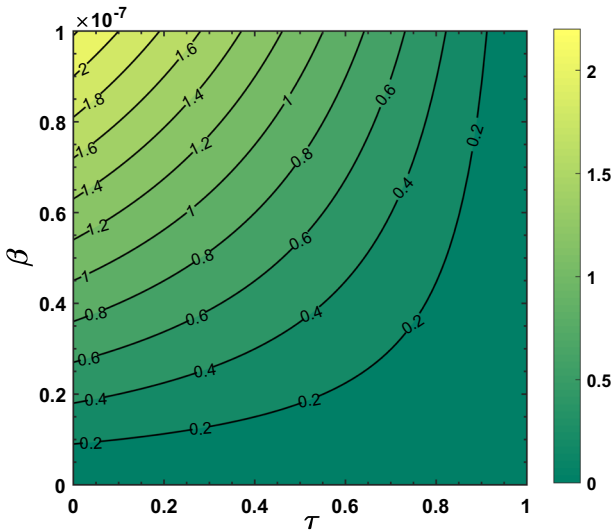


Fig. 9 Contour plot of the basic reproductive number \mathcal{R}_0 as a function of vaccine efficacy ($\tau \in [0, 1]$) and measles contact rate ($\beta \in [0, 1e - 07]$), whereas the remaining parameters are taken from Table 2

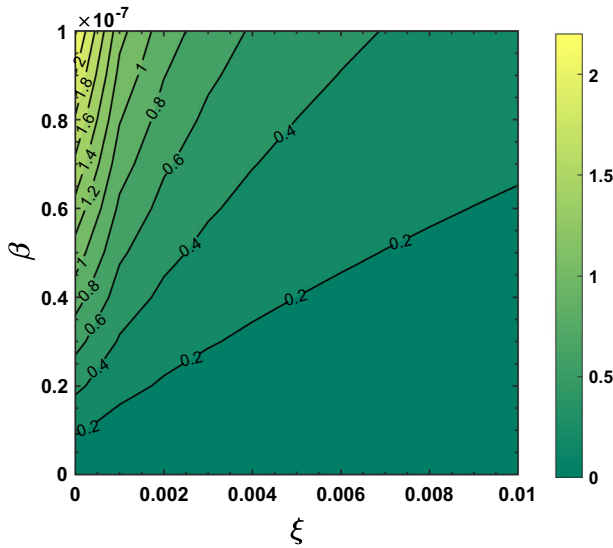
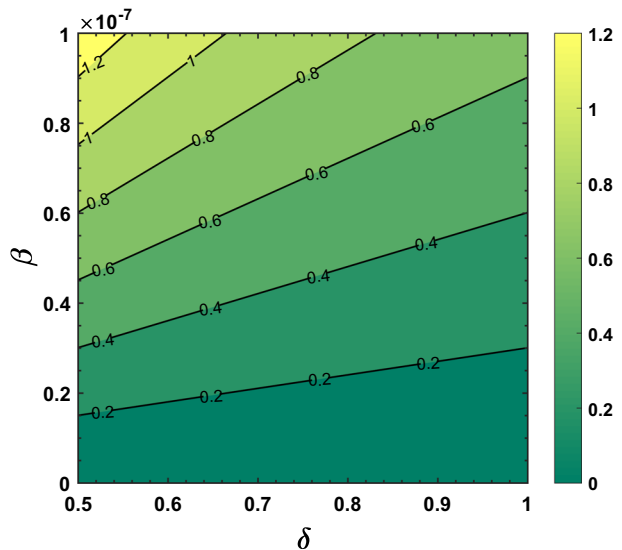


Fig. 10 Contour plot of the basic reproductive number \mathcal{R}_0 as a function of vaccine coverage rate ($\xi \in [0, 0.01]$) and measles contact rate ($\beta \in [0, 1e - 07]$), whereas the remaining parameters are taken from Table 2

Fig. 11 Contour plot of the basic reproductive number \mathcal{R}_0 as a function of recovery rate ($\delta \in [0.5, 1]$) and measles contact rate ($\beta \in [0, 1e - 07]$), whereas the remaining parameters are taken from Table 2



8 Future directions

In future, we aim to work on fractional-order versions of the measles model proposed in this paper and solve them using the techniques followed in [47–50]. Fractional-order operators including Weyl, Riesz, Riemann–Liouville, Caputo, Caputo–Fabrizio, Atangana–Baleanu, Atangana–Gomez, fractal–fractional and others have capability to capture complex and anomalous behavior of dynamical systems that describe a physical or natural phenomenon.

Fig. 12 Contour plot of the basic reproductive number \mathcal{R}_0 as a function of rate of developing clinical symptoms ($\alpha \in [0, 1]$) and measles contact rate ($\beta \in [0, 1e-06]$), whereas the remaining parameters are taken from Table 2

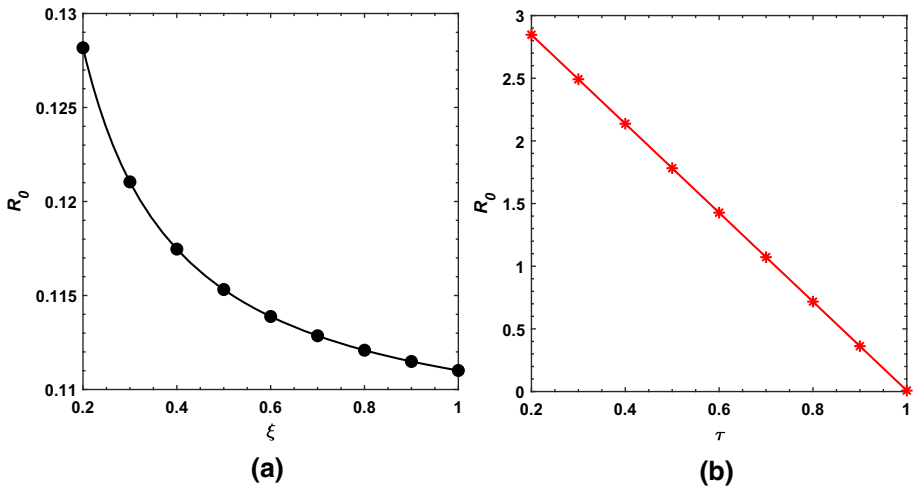
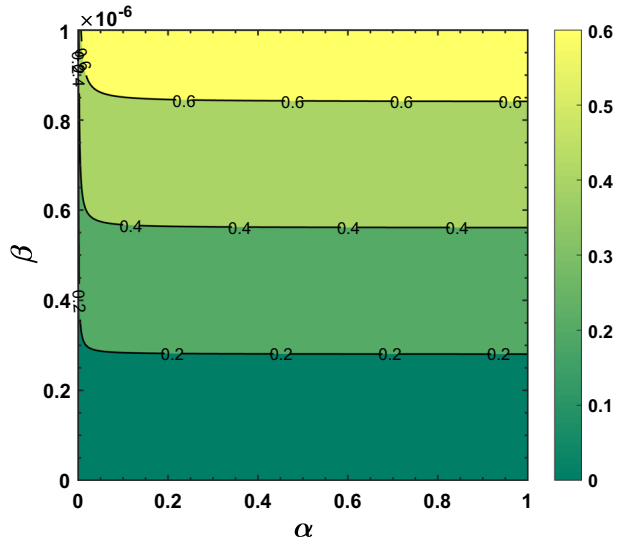


Fig. 13 Behavior of the basic reproductive number \mathcal{R}_0 for increasing values of **a** vaccine coverage rate $\xi \in [0.2, 1]$ and **b** efficacy of vaccine $\tau \in [0.2, 1]$

The non-local nature of these operators retains memory of the underlying processes which proves to be fruitful in case of epidemiological models since such models are designed to comprehend transmission dynamics of an epidemic which, in turn, has characteristics of memory. Thus, the future works will be devoted to the use of the above operators from fractional calculus for improving the measles system introduced in the present research study.

Data Availability Statement This manuscript has associated data in a data repository. [Authors' comment: The data used in this study is taken from Measles monthly bulletin published on World Health Organization website (<http://www.emro.who.int/vpi/publications/measles-monthly-bulletin.html>). See reference [36].]

Compliance with ethical standards

Conflict of interest The authors declare that they have no conflict of interest.

Funding This research did not receive any specific grant from funding agencies in the public, commercial or not-for-profit sectors.

References

1. Y. Yanagi, M. Takeda, S. Ohno, Measles virus: cellular receptors, tropism and pathogenesis. *J. Gen. Virol.* **87**(10), 2767–2779 (2006)
2. D. Griffin, The immune response in measles: virus control, clearance and protective immunity. *Viruses* **8**(10), 282 (2016)
3. R.T. Perry, N.A. Halsey, The clinical significance of measles: a review. *J. Infect. Dis.* **189**(Supplement–1), S4–S16 (2004)
4. L.G. Dales, K.W. Kizer, G.W. Rutherford, C.A. Pertowski, S.H. Waterman, G. Woodford, Measles epidemic from failure to immunize. *West. J. Med.* **159**(4), 455 (1993)
5. <https://www.the-scientist.com/news-opinion/measles-epidemic-rocks-madagascar-65442>
6. <https://www.who.int/immunization/diseases/measles/en/>
7. World Health Organization, Eastern Mediterranean Vaccine Action Plan 2016–2020: a framework for implementation of the Global Vaccine Action Plan (No. WHO-EM/EPI/353/E). World Health Organization, Regional Office for the Eastern Mediterranean (2019)
8. <https://www.dawn.com/news/1520931>
9. M.O. Mere, J.L. Goodson, A.K. Chandio, M.S. Rana, Q. Hasan, N. Teleb, J.P. Alexander Jr., Progress toward measles elimination—Pakistan, 2000–2018. *Morb. Mortal. Wkly. Rep.* **68**(22), 505 (2019)
10. A.A. Momoh, M.O. Ibrahim, I.J. Uwanta, S.B. Manga, Mathematical model for control of measles epidemiology. *Int. J. Pure Appl. Math.* **87**(5), 707–717 (2013)
11. S.O. Adewale, I.T. Mohammed, I.A. Olopade, Mathematical analysis of effect of area on the dynamical spread of measles. *IOSR J. Eng.* **4**(3), 43–57 (2014)
12. R. Smith, A. Archibald, E. MacCarthy, L. Liu, N.S. Luke, A mathematical investigation of vaccination strategies to prevent a measles epidemic. *NCJ Math. Stat.* **2**, 29–44 (2016)
13. S.M. Garba, M.A. Safi, S. Usaini, Mathematical model for assessing the impact of vaccination and treatment on measles transmission dynamics. *Math. Methods Appl. Sci.* **40**(18), 6371–6388 (2017)
14. O.J. Peter, O.A. Afolabi, A.A. Victor, C.E. Akpan, F.A. Oguntolu, Mathematical model for the control of measles. *J. Appl. Sci. Environ. Manag.* **22**(4), 571–576 (2018)
15. L.K. Beay, Modelling the effects of treatment and quarantine on measles, in *AIP Conference Proceedings* (Vol. 1937, No. 1, p. 020004). AIP Publishing LLC (2018)
16. F. Ashraf, M.O. Ahmad, Nonstandard finite difference scheme for control of measles epidemiology. *Int. J. Adv. Appl. Sci.* **6**(3), 79–85 (2019)
17. D. Aldila, D. Asrianti, A deterministic model of measles with imperfect vaccination and quarantine intervention, in *Journal of Physics: Conference Series*, Vol. 1218, No. 1. (IOP Publishing 2019, May), p. 012044
18. A. Bashir, M. Mushtaq, Z.U.A. Zafar, K. Rehan, R.M.A. Muntazir, Comparison of fractional order techniques for measles dynamics. *Adv. Differ. Equa.* **2019**(1), 334 (2019)
19. H.W. Berhe, O.D. Makinde, Computational modelling and optimal control of measles epidemic in human population. *Biosystems* **190**, 104102 (2020)
20. H. Alhamami, A Susceptible-Exposed-Infected-Recovered-Vaccinated (SEIRV) Mathematical Model of Measles in Madagascar (Doctoral dissertation, Morgan State University) (2019)
21. F.M.G. Magpantay, A.A. King, P. Rohani, Age-structure and transient dynamics in epidemiological systems. *J. R. Soc. Interface* **16**(156), 20190151 (2019)
22. J. Huang, S. Ruan, X. Wu, X. Zhou, Seasonal transmission dynamics of measles in China. *Theory Biosci.* **137**(2), 185–195 (2018)

23. W. Yang, J. Li, J. Shaman, Characteristics of measles epidemics in China (1951–2004) and implications for elimination: a case study of three key locations. *PLoS Comput. Biol.* **15**(2), e1006806 (2019)
24. M.O. Fred, J.K. Sigey, J.A. Okello, J.M. Okwoyo, G.J. Kang'ethe, Mathematical modeling on the control of measles by vaccination: case study of KISII County, Kenya. *SIJ Trans. Comput. Sci. Eng. Appl. (CSEA)* **2**, 61–69 (2014)
25. S. Okyere-Siabouh, I.A. Adetunde, Mathematical Model for the study of measles in Cape Coast Metropolis. *Int. J. Modern Biol. Med.* **4**(2), 110–133 (2013)
26. G. Hooker, S.P. Ellner, L.D.V. Roditi, D.J. Earn, Parameterizing state-space models for infectious disease dynamics by generalized profiling: measles in Ontario. *J. R. Soc. Interface* **8**(60), 961–974 (2011)
27. P. Manfredi, J.R. Williams, Realistic population dynamics in epidemiological models: the impact of population decline on the dynamics of childhood infectious diseases: Measles in Italy as an example. *Math. Biosci.* **192**(2), 153–175 (2004)
28. S.C. Chen, C.F. Chang, L.J. Jou, C.M. Liao, Modelling vaccination programmes against measles in Taiwan. *Epidemiol. Infect.* **135**(5), 775–786 (2007)
29. S.O. Sowole, D. Sangare, A.A. Ibrahim, I.A. Paul, On the existence, uniqueness, stability of solution and numerical simulations of a mathematical model for measles disease. *Int. J. Adv. Math.* **2019**(4), 84–111 (2019)
30. A. Cilli, K. Ergen, E. Akat, Some mathematical models and applications used in epidemics. *SIGMA J. Eng. Nat. Sci.* **37**(1), 17–23 (2019)
31. R. Almeida, S. Qureshi, A fractional measles model having monotonic real statistical data for constant transmission rate of the disease. *Fractal Fract.* **3**(4), 53 (2019)
32. S. Qureshi, Effects of vaccination on measles dynamics under fractional conformable derivative with Liouville–Caputo operator. *Eur. Phys. J. Plus* **135**(1), 63 (2020)
33. S. Qureshi, Real life application of Caputo fractional derivative for measles epidemiological autonomous dynamical system. *Chaos Solitons Fract.* **134**, 109744 (2020)
34. S. Qureshi, Z. Memon, Monotonically decreasing behavior of measles epidemic well captured by Atangana–Baleanu–Caputo fractional operator under real measles data of Pakistan. *Chaos Solitons Fract.* **131**, 109478 (2020)
35. A. Wesolowski, A. Winter, A.J. Tatem et al., Measles outbreak risk in Pakistan: exploring the potential of combining vaccination coverage and incidence data with novel data-streams to strengthen control. *Epidemiol. Infect.* **146**, 1575–1583 (2018)
36. World Health Organization, Measles monthly bulletin. <http://www.emro.who.int/vpi/publications/measles-monthly-bulletin.html>. Accessed 21 December (2019)
37. P. Van den Driessche, J. Watmough, Reproduction numbers and sub-threshold endemic equilibria for compartmental models of disease transmission. *Math. Biosci.* **180**(1–2), 29–48 (2002)
38. R. Anguelov, S.M. Garba, S. Usaini, Backward bifurcation analysis of epidemiological model with partial immunity. *Comput. Math. Appl.* **68**(9), 931–940 (2014)
39. S.S. Musa, S. Zhao, H.S. Chan, Z. Jin, D. He, *A Mathematical Model to Study the 2014–2015 Large-Scale Dengue Epidemics in Kaohsiung and Tainan Cities in Taiwan* (China, Mathematical Biosciences and Engineering, 2019)
40. J.P. LaSalle, *The Stability of Dynamical Systems*, vol. 25 (SIAM, Philadelphia, 1976)
41. D.A. Rand, Mapping global sensitivity of cellular network dynamics: sensitivity heat maps and a global summation law. *J. R. Soc. Interface* **5**(suppl–1), S59–S69 (2008)
42. S. Marino, I.B. Hogue, C.J. Ray, D.E. Kirschner, A methodology for performing global uncertainty and sensitivity analysis in systems biology. *J. Theor. Biol.* **254**(1), 178–196 (2008)
43. J.C. Helton, F.J. Davis, Illustration of sampling-based methods for uncertainty and sensitivity analysis. *Risk Anal.* **22**(3), 591–622 (2002)
44. M.D. Morris, Factorial sampling plans for preliminary computational experiments. *Technometrics* **33**(2), 161–174 (1991)
45. I.Y.M. Sobol', On sensitivity estimation for nonlinear mathematical models. *Matematicheskoe Modelirovanie* **2**(1), 112–118 (1990)
46. H.W. Berhe, O.D. Makinde, D.M. Theuri, Parameter estimation and sensitivity analysis of dysentery diarrhea epidemic model. *J. Appl. Math.* (2019). <https://doi.org/10.1155/2019/8465747>
47. O.A. Arqub, N. Shawagfeh, Application of reproducing kernel algorithm for solving Dirichlet time-fractional diffusion-Gordon types equations in porous media. *J. Porous Media* **22**(4), 411–434 (2019)
48. O. Abu Arqub, Application of residual power series method for the solution of time-fractional Schrödinger equations in one-dimensional space. *Fundamenta Informaticae* **166**(2), 87–110 (2019)
49. O.A. Arqub, Numerical solutions of systems of first-order, two-point BVPs based on the reproducing kernel algorithm. *Calcolo* **55**(3), 31 (2018)

50. O. Abu Arqub, Numerical algorithm for the solutions of fractional order systems of Dirichlet function types with comparative analysis. *Fundamenta Informaticae* **166**(2), 111–137 (2019)